Received: 30 January 2018 | Revised: 5 April 2018 | Accepted: 4 July 2018 | Published on: 28 November 2018

DOI: 10.1002/met.1753

Meteorological Applications RMetS

RESEARCH ARTICLE

Evaluation of a neuro-fuzzy technique in estimating pan evaporation values in low-altitude locations

Jalal Shiri

Water Engineering Department, Faculty of Agriculture, University of Tabriz, Tabriz, Iran

Correspondence
Jalal Shiri, Water Engineering Department, Faculty of Agriculture, University of Tabriz, Tabriz, Iran.
Email: j_shiri2005@yahoo.com

The evaporation of water from free-water surfaces or land surfaces is one of the main components of the hydrological cycle and is a complex outcome of various meteorological and physical parameters. A simulation procedure was evaluated in this paper to study the capabilities of a neuro-fuzzy (NF) technique to estimate daily pan evaporation (E_P) magnitudes using meteorological variables. The assessment of the NF technique for simulating E_P values was performed *via* local (temporal) and external (spatial) data-management scenarios. Hence, a thoroughgoing scan of the possible train and test-set combinations was carried out based on the temporal and spatial criteria using *k*-fold testing procedures. A comparison was also made between the NF and neural networks (NN) methods using the same data and procedures. The obtained outcomes revealed that the proposed generalized NF and NN models have good abilities at simulating E_P values using meteorological data. Therefore, the calibration of local NF models might not be required if sufficient meteorological parameters exist in other weather stations. The results also demonstrated that a proper assessment of the models' performance accuracy should include a complete temporal/spatial scanning of the used patterns.

KEYWORDS
external models, local models, neural networks, neuro-fuzzy, pan evaporation

1 | INTRODUCTION

Water evaporation (an irreversible phenomenon) is one of the important elements of the hydrological cycle (Brutsaert, 1982). Evaporation from the land surface is the largest element of the terrestrial hydrologic cycle (Wallace, 1995), which uses about 61% of total precipitation (Chow *et al*., 1988). Therefore, it is an important element of the hydrologic cycle and accurate estimation of its quantity is a crucial subject in hydrology, agro-meteorology and irrigation engineering. Numerous studies have been carried out to derive the mathematical/empirical relationships between the evaporation and meteorological factors (e.g. Kohler *et al*., 1955; Stephen and Stewart, 1963; Griffiths, 1966; Linarce, 1967; Priestley and Taylor, 1972; Burman, 1976; de Bruin, 1978). However, such empirical relationships have their downside because they are non-transferable (Cahoon *et al*., 1991). Evaporation is a nonlinear phenomenon that needs more robust models to be simulated using meteorological parameters. Therefore, the application of data-driven models (e.g. the neuro-fuzzy (NF) technique) might be a suitable alternative to the empirical models (Kim *et al*., 2015).

The NF technique is a combination of an adaptive neural network (NN) and a fuzzy inference system (FIS), where the FIS parameters are identified by the NN-learning algorithms. The NF technique can approximate any real continuous function on a compact set (Jang *et al*., 1997). It also classifies a parameter set *via* a hybrid learning rule by merging the back-propagation gradient descent error digestion and a least squares error method. Two fuzzy approaches: the Mamdani (Mamdani and Assilian, 1975) and the Sugeno (Takagi and Sugeno, 1985), can be used in different disciplines. The main difference between them is that they belong to the consequent part: where Mamdani's approach uses the

fuzzy membership functions (MFs), Sugeno's approach applies linear or constant functions. Sugeno's fuzzy approach (Takagi and Sugeno, 1985) was applied in the present paper to find the output variable (E_P) magnitudes by using the input variables (meteorological data). Among others, Keskin *et al*. (2004), Kisi (2006a), Kisi and Ozturk (2007), Aytek (2008), Shiri *et al*. (2011) and Pour Ali Baba *et al*. (2013) employed the NF technique to model evaporation. Kisi and Shiri (2010) used the NF techniques to predict short-/long-term stream flows. Shiri and Kisi (2011a) compared genetic programming with the NF to predict groundwater table variations. Shiri and Kisi (2011b) compared genetic programming and the NF to simulate pan evaporation magnitudes using real-time and estimated meteorological parameters.

An NN has one or more hidden layers, whose computation nodes are called "hidden neurons". The hidden neurons intervene between the external input and the network output in some useful manner. The network is enabled to extract higher order statistics by adding one or more hidden layers (Haykin, 1998). Kisi (2006b, 2006c) applied the NN to estimate evaporation.Most of these NF employments have adopted a simple data set assignment where the training and test blocks have been defined chronologically. However, some others tried to apply other data-management scenarios (e.g. Kumar *et al*., 2009; Marti and Gasque, 2010; Kisi *et al*., 2012; Wang *et al*., 2014; Shiri *et al*., 2014a). Martí *et al*. (2011) argued that a simple data set assignment might derive in misleading/partially valid statements. The present research aimed to evaluate the performance accuracy of the NF and NN models when estimating E_P using both spatial and temporal data-management scenarios with daily meteorological data from four low-altitude weather stations in United States. The regional variations in temperature and rainfall magnitudes and patterns in the lowlands supply fundamental information in order to understand the climatic variability that provides important differences in vegetation and primary production (Coppok, 1994). Hence, the present paper evaluated the performance accuracy of the models in lowland regions. Therefore, complete data set scanning was carried out by defining all possible training and test combinations based on temporal and spatial criteria. This is very important from the practical point of view because it exempts one from using the local data for evaporation modelling by using the spatially evaluated models. Therefore, the regions with limited or missing data would be benefit from using the spatial (external) models.

2 | MATERIALS AND METHODS

2.1 | Data set

Daily meteorological data from four automated weather stations in the United States were used. Table 1 presents the geographical positions of the weather stations. The minimum and maximum station elevations above mean sea level were for San Diego (4 masl) and Fresno (102 masl), which shows that the altitude difference between the stations was small. The considered variables were daily air temperature (T_A), solar radiation (R_S), relative humidity (R_H), wind speed (W_S) and pan evaporation (E_P) for a 10-year period (January 1981–December 1990). Table 2 sums up the daily statistical parameters of the used parameters, where X_{mean}, X_{max}, X_{min}, S_X, C_V and C_{SX} are the mean, maximum, minimum, standard deviation, co-efficient of variation and skewness co-efficient respectively. All the studied locations show similar statistical parameters for the meteorological variables, although some obvious differences, especially in terms of the higher order momentums (skewness), were obvious between the stations. Such differences might affect the extrapolations of E_P using the NF models.

2.2 | Neuro-fuzzy (NF) system

As a simple example, suppose an FIS with two inputs x and y and one output f. The first-order Sugeno fuzzy model can be given as:

$$\text{Rule 1: If } x \text{ is } A_1 \text{ and } y \text{ is } B_1, \text{ then } f_1 = p_1x + q_1y + r_1 \quad (1)$$

$$\text{Rule 2: If } x \text{ is } A_2 \text{ and } y \text{ is } B_2, \text{ then } f_2 = p_2x + q_2y + r_2 \quad (2)$$

where A_1, A_2 and B_1, B_2 are the MFs for inputs x and y respectively; and p_1, q_1, r_1 and p_2, q_2, r_2 are the parameters of the output function. Here, the output f is the weighted average of the individual rule outputs and is a crisp value.

The output of the i-th node in layer l is shown as $O_{l,i}$. Each node i in layer 1 is an adaptive node with node $O_{l,\,i} = \phi A_i(x)$, for $i = 1, 2$, or $O_{l,\,i} = \phi B_{i-2}(y)$, for $i = 3, 4$, where x (or y) is the input to the i-th node; and A_i (or B_{i-2}) is a linguistic label (such as "low" or "high") associated with this node. The MFs for A and B are generally described by generalized bell functions, for example:

$$\phi A_i(x) = \frac{1}{1 + [(x - c_i)/a_i]^{2b_i}} \quad (3)$$

where $\{a_i, b_i, c_i\}$ is the parameter set. Parameters in this layer are called premise parameters. The outputs of this layer are the membership values of the premise part. Layer 2 includes the nodes labelled Π that multiply incoming signals, then send the product out. For instance:

$$O_{2,i} = w_i = \phi A_i(x)\phi B_i(y), \quad i = 1, 2. \quad (4)$$

Each node output shows the firing strength of a rule. The nodes labelled "N" compute the ratio of the i-th rule's firing strength to the sum of all rules' firing strengths in layer 3:

$$O_{3,i} = \overline{w}_i = \frac{w_i}{w_1 + w_2}, \quad i = 1, 2. \quad (5)$$

TABLE 1 Summary of the geographical positions of the studied locations

Station	Station code	US state	Latitude (° N)	Longitude (° W)	Altitude (masl)
Fresno	1	California	36.78	119.72	102
Los Angles	2	California	33.56	118.24	30
San Diego	3	California	32.44	117.10	4
Santa Maria	4	California	34.54	120.27	77

The outputs of this layer are called normalized firing strengths. The nodes of layer 4 are adaptive with node functions:

$$O_{4,i} = \overline{w}_i f_i = \overline{w}_i (p_i x + q_i y + r_i) \quad (6)$$

where $\overline{w}_i$ is the output of layer 3; and $\{p_i, q_i, r_i\}$ is the parameter set. Parameters of this layer are called consequent parameters. The single fixed node of layer 5 labelled Σ calculates the final output as the summation of all incoming signals:

$$O_{5,i} = \sum_{i=1} \overline{w}_i f_i = \frac{\sum_i w_i f_i}{\sum_i w_i} \quad (7)$$

Hence, an adaptive network that is functionally equivalent to a Sugeno first-order FIS was built. For detailed information about the adaptive-network-based fuzzy inference system (ANFIS), see Jang (1993).

2.3 | Neural networks (NN)

In the present study, NN models were trained by using a Levenberg–Marquardt algorithm because this is more powerful and faster than the conventional gradient-descent technique (Hagan and Menhaj, 1994). Moreover, a single hidden layer would be enough for the NN to approximate the nonlinear phenomenon (Cybenco, 1989). Therefore, a single-hidden-layer NN was employed and the numbers of hidden neurons were determined iteratively. The sigmoid and linear functions were used as the activation functions of the hidden and output nodes respectively.

2.4 | Modelling protocol

According to Griffiths (1966), most of the evaporation variations can be associated with air temperature and wind speed changes. In the present study, the following input

TABLE 2 Statistical parameters of the used data set

Station	Parameter	Unit	X_{max}	X_{min}	X_{mean}	S_X	C_V	C_{SX}
Fresno	T_A	°C	34.900	–3.000	17.801	8.118	0.456	0.010
	W_S	m/s	9.913	0.273	3.081	1.299	0.422	0.673
	R_H	%	32.963	1.467	18.512	8.783	0.474	–0.135
	R_S	MJ/m^2 day	100.000	18.000	52.151	19.010	0.365	0.478
	P	KPa	102.300	98.300	100.440	0.512	0.005	0.351
	E_P	mm	18.200	0.000	6.242	4.475	0.717	0.337
Los Angeles	T_A	°C	29.900	5.700	17.011	3.343	0.197	0.038
	W_S	m/s	12.719	1.439	3.604	0.973	0.270	2.029
	R_H	%	31.191	2.771	17.928	6.846	0.382	–0.018
	R_S	MJ/m^2 day	102.700	99.100	101.170	0.368	0.004	0.143
	P	KPa	99.000	9.000	63.638	15.745	0.247	–1.088
	E_P	mm	14.600	0.400	4.745	1.935	0.408	0.400
San Diego	T_A	°C	30.200	7.200	18.029	3.485	0.193	0.146
	W_S	m/s	10.897	0.961	3.704	0.989	0.267	1.152
	R_H	%	31.066	3.277	18.100	6.618	0.366	0.022
	R_S	MJ/m^2 day	102.800	99.500	101.445	0.346	0.003	0.160
	P	KPa	97.000	10.000	64.915	14.120	0.218	–1.280
	E_P	mm	14.800	0.000	4.851	1.872	0.386	0.318
Santa Maria	T_A	°C	26.700	0.500	13.635	3.410	0.250	–0.112
	W_S	m/s	12.530	0.810	4.592	1.535	0.334	0.515
	R_H	%	31.923	3.285	18.575	7.239	0.390	–0.045
	R_S	MJ/m^2 day	102.300	98.600	100.795	0.374	0.004	0.027
	P	KPa	95.000	16.000	63.478	13.639	0.215	–0.795
	E_P	mm	24.000	0.000	5.322	2.790	0.524	0.569

configurations were assessed, which imply the effect of air temperature (T_A), wind speed (W_S) and solar radiation (R_S) on total E_P magnitudes:

- T_A and W_S
- T_A and R_S
- T_A, W_S, R_H and R_S

It is very important to introduce the input–output matrices to the applied models in such a way that the generalizability of the models can be assessed. In the present paper, the evaluation of the NF models' performance accuracies was performed using local (LNF models) and external (ENF models) *k*-fold testing cross-validation. Therefore, in the LNF models, the minimum temporary test period was fixed as one year. The models were then trained using the data from the remaining nine years. The process was repeated at each station till all the existing years were involved in the train-test phases. As the present study uses data from four stations during the 10 years, a total 120 (4 stations*10 years*3 input configurations) train-test phases were established for the LNF models. Further, in the ENF models, the available patterns of three stations were used as training data, while the developed models were tested using the complete patterns of one station. Therefore, a total 12 (4 stations*3 input configurations) train-test procedures were involved for the ENF models.

Four statistical measures, namely, the co-efficient of determination (r^2), scatter index (SI), mean absolute error (MAE) and co-efficient of residual mass (CRM), were used to evaluate the performance accuracy of the LNF and ENF models, the expressions for which are as follows:

$$r^2 = \left[\frac{\sum_{i=1}^{n}\left(E_o-\overline{E}_o\right)\left(E_M-\overline{E}_M\right)}{\sqrt{\sum_{i=1}^{n}\left(E_o-\overline{E}_o\right)^2\sum_{i=1}^{n}\left(E_M-\overline{E}_M\right)^2}}\right]^2 \quad (8)$$

$$SI = \frac{RMSE}{\overline{E}_0} = \frac{\sqrt{\frac{1}{n}\sum_{i=1}^{n}\left(E_M-E_o\right)^2}}{\overline{E}_0} \quad (9)$$

$$MAE = \frac{\sum_{i=1}^{n} abs\left(E_o-E_M\right)}{n} \quad (10)$$

$$CRM = \frac{\left(\sum_{i=1}^{n}E_o-\sum_{i=1}^{n}E_M\right)}{\sum_{i=1}^{n}E_o} \quad (11)$$

where E_o denotes the measured evaporation value at the *i*-th time step; E_M is the corresponding estimated evaporation value; *n* is the number of patterns; $\overline{E}_O$ is the mean value of the measured evaporation values; and $\overline{E}_M$ is the mean value of the estimated evaporation values. The statistical indices of the LNF models belonged to the complete period in each station, that is, the estimations of each test stage were pooled together chronologically and the statistical parameters were computed for the complete period.

3 | RESULTS AND DISCUSSION

The statistical indices of the LNF, LNN, ENF and ENN models averaging the results of the all stations are shown in Table 3. As could be foreshadowed, the quadruple-input models (LNF3 and ENF3 as well as LNN3 and ENN3) gave the best performance accuracy. Nevertheless, the major downside of this input combination is the requirement of more input variables that might not be provided in many areas. Moreover, the local models produced more accurate outcomes than the external models, since they were trained

TABLE 3 Global average performance parameters of the considered approaches

Model	Co-efficient of determination (r^2)	Mean absolute error (MAE) (mm)	Scatter index (SI)	Co-efficient of residual mass (CRM)
Local				
NF1	0.590	1.179	0.280	–0.005
NF2	0.756	0.845	0.215	–0.003
NF3	0.977	0.212	0.052	–0.0003
NN1	0.531	1.296	0.308	–0.005
NN2				
NN3				
External				
NF1	0.541	1.290	0.400	0.010
NF2	0.720	1.160	0.330	0.030
NF3	0.856	0.792	0.170	0.005
NN1	0.487	1.421	0.442	0.013
NN2				
NN3				

with the meteorological patterns of the same stations that were used for testing (using different years for training and for testing). In the case of the external models, the ENF3 (which relied on input combination 3) improved the performance accuracy of the LNF1 and LNF2 models by 40% and 21% reductions in their SI values respectively. Finally, the models that relied on T_A and R_S were more accurate than those that relied on T_A and W_S. Therefore, the inclusion of R_S as an input variable of the NF models (instead of W_S) seems to be more suitable in simulating E_P, which confirms the results obtained by Shiri *et al.* (2014b).

Figures 1–3 show the performance indicators *per* test station for the input combinations 1–3 respectively. By comparing Figures 1–3, the above-mentioned statements regarding the superiority of the LNF3, LNN3, ENF3 and ENN3 models over the other two applied input combinations can be confirmed. Regarding the input combination 1, the local model (LNF1) gave the most accurate results in Fresno (code: 1; with the highest altitude) with the minimum SI (0.17) and MAE (1.004 mm/day) and the highest r^2 (0.916) values, while Santa Maria (code: 4) presented the worst results for this input combination with the highest SI (0.38) and MAE (1.51 mm/day) as well as the lowest r^2 (0.481) values. A possible reason for such a discrepancy between the stations would be the differences in the statistical characteristics (Table 2) of the meteorological data (especially in terms of T_A and W_S) of the stations. Further, this might show the differences among the different subseries of the meteorological parameters used for training and testing the models, which makes it difficult to obtain accurate results in some locations. In the case of the external model (ENF), the best simulations corresponded to Los Angles (code: 2) with the lowest SI (0.31) and MAE (1.09) values, while the simulations obtained in Santa Maria (code: 4) were the worst among the others with the highest SI and MAE values (0.48 and 1.42 mm/day respectively). Again, Santa Maria presented the worst results for the ENF model, such as the local one. This might be attributed to its disimilarities in terms of the time-series trend of the meteorological parameters with the other studied locations. The r^2 value of the ENF model for Los Angles was lower than that for the Fresno, although an adverse outcome was observed for the MAE and SI values. This could be expected in some cases, since the r^2 value presents only the linear relations between the target-simulation pairs, so some vast differences would not be pictured well with this index if they had a similar trend in variations. A similar statement could also be presented for the NN models.

Attending to the input combination 2 (LNF2 and ENF2 models; Figure 2), Fresno gave the best simulations (SI = 0.14, MAE = 0.649 mm/day), while Santa Maria presented the lowest performance accuracy (SI = 0.29, MAE = 1.19 mm/day), similar to input combination 1. The simulations for San Diego (code: 3; with the lowest altitude) were similar to those for Fresno (ΔSI = 0.57, ΔMAE = 0.063 mm/day), which might be linked to the similarities

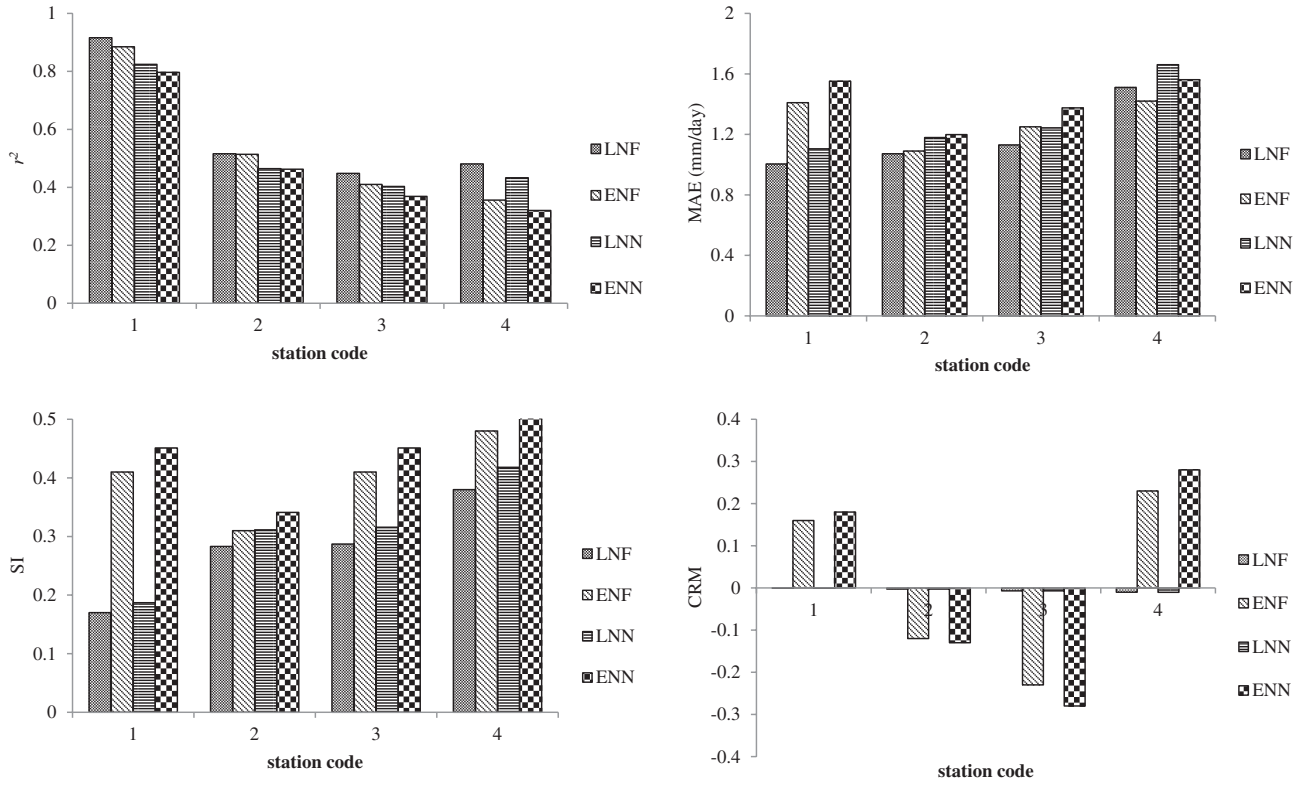

FIGURE 1 Error statistics for the local neuro-fuzzy (LNF), local neural network (LNN), external neuro-fuzzy (ENF) and external neural network (ENN) models relying on input combination

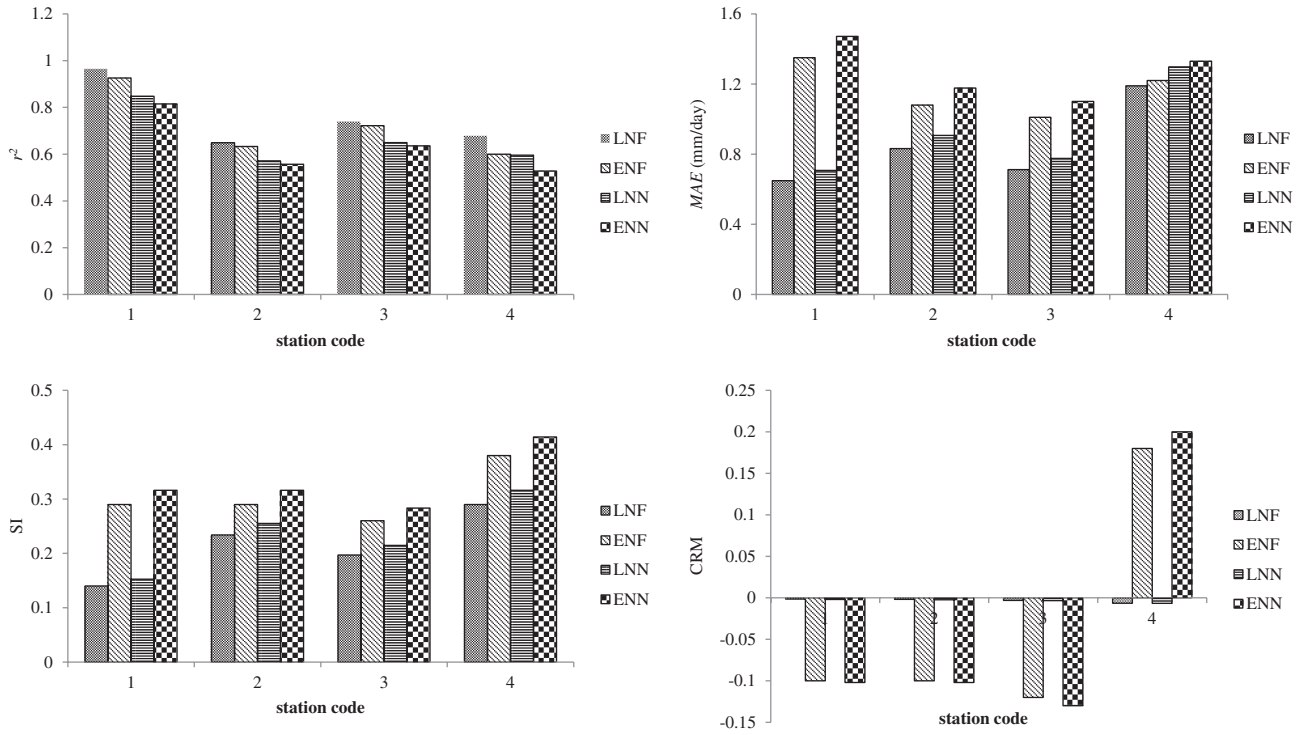

FIGURE 2 Error statistics for the local neuro-fuzzy (LNF), local neural network (LNN), external neuro-fuzzy (ENF) and external neural network (ENN) models relying on input combination 2

between the E_P statistics (Table 2) of these stations. A comparison of the present input combination with the former (combination 1) showed that the LNF2 and ENF2 have improved the accuracy of the LNF1 and ENF1 models (in Fresno) with 17% and 29% reduction in SI values respectively. The higher performance improvement belonged to the external models, which could show the effect of including the most influential parameters (here, R_S) in externally trained models of E_P simulation. The same performance improvements in terms of SI reduction in Santa

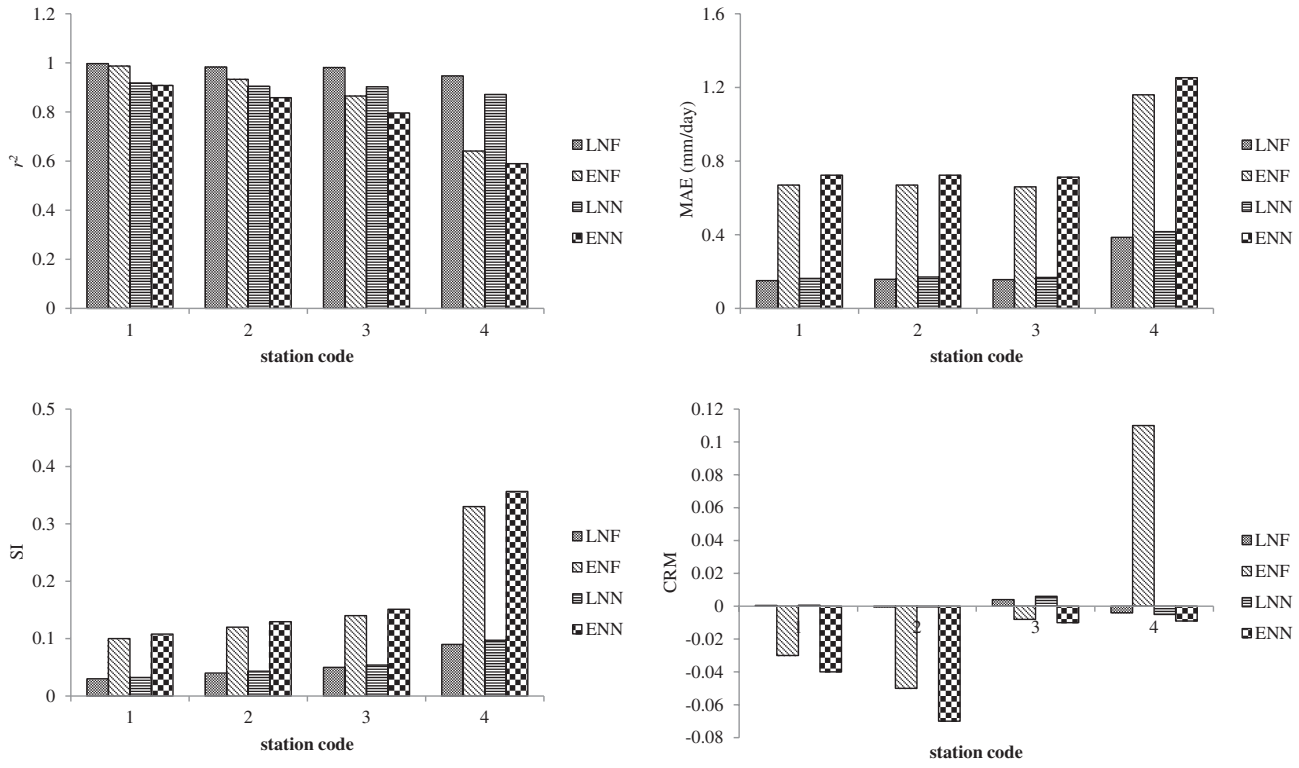

FIGURE 3 Error statistics for the local neuro-fuzzy (LNF), local neural network (LNN), external neuro-fuzzy (ENF) and external neural network (ENN) models relying on input combination 3

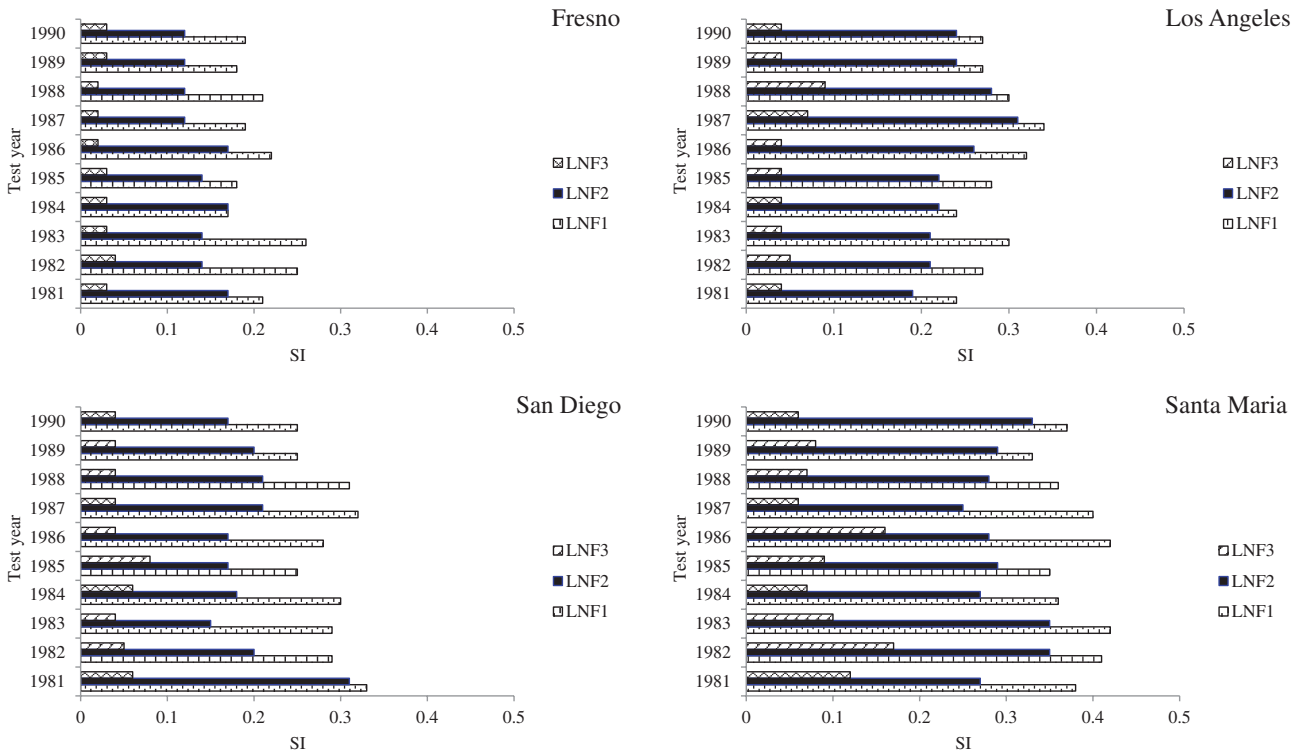

FIGURE 4 Breakdown of annual scatter index (SI) values of the local neuro-fuzzy (LNF) models at each station [Colour figure can be viewed at wileyonlinelibrary.com [Colour figure can be viewed at wileyonlinelibrary.com]

Maria were 23% and 21% respectively. Here, the local model presented more improvement than the external one. Again, the statements given above would stand here regarding the disimilarities between the time-series of the used meteorological parameters of the studied stations.

Finally, in the case of input combination 3, Fresno and Santa Maria again presented the best and worst outcomes with the lowest and highest SI and MAE values respectively. The LNF3 model improved the performance accuracy of the LNF2 model with 78% and 77% reductions in the SI and MAE values of Fresno respectively, as well as 69% and 67% reductions in the same respective indicators for Santa Maria. This shows that the inclusion of all necessary variables as input parameters enhanced modelling accuracy to a great extent, although the need for large amount of meteorological variables would be a crucial drawback of this model, as discussed by Shiri *et al.* (2014b). Therefore, the assessment of the NF models based on external patterns (ancillary data from other stations which have not been incorporated in training phase) would be necessary. Analysis of the statistics of the ENF3 model shows SI reductions of 65%, 58%, 46% and 13% for Fresno, Los Angeles, San Diego and Santa Maria respectively when compared with those of the ENF2 model. Again, the minimum performance improvement belonged to Santa Maria. Comparing Figures 1–3 shows that the ENF3 improved the local NF models' (LNF1 and LNF2) accuracies in terms of both SI and MAE reductions. The CRM and r^2 values fluctuated between the models and stations. However, as a general statement, a global increase in model accuracy could be observed, as stated above. Such oscillations among locations dictated the necessity of evaluating the models' performance accuracy *via* complete data set-scanning processes, as discussed by Martí *et al.* (2011).

Figure 4 illustrates the breakdown of the annual SI values for the LNF models at each studied location. The SI magnitudes show obvious fluctuations within the test years for all three input combinations and four studied stations. Among others, the mean maximum fluctuations for the SI during the study period were observed for Los Angeles (0.1), San Diego (0.16) and Santa Maria (0.16) for input combinations 1–3 respectively. The fluctuations range was at a minimum for Fresno. The order of the models' performance accuracy (in terms of SI) was almost the same for all stations and test years, where input combination 3 surpasses inputs 1 and 2, and input 2 surpasses the first input combination. Differences between the mean SI values for the applied input combinations at each station are obvious, emphasizing the superiority of the third input combination over the two other applied combinations. However, considerable oscillations could be observed in the SI values for different test years, as stated above. Therefore, a complete data-scanning procedure is a crucial data handling method for managing the E_P modelling issues.

Summarizing, the NF and NN models had good capability at modelling daily E_P values using even limited meteorological inputs (T_A and R_S) in low-altitude stations, which might have different climatic characteristics in terms of meteorological variables than the other regions. Wind

turbulence effects are more obvious in those regions. This was the reason why the wind speed-based models (based on mass-transfer-based theory) could not give promising results for those regions. Further studies might be needed to enhance the outcomes of the present study.

4 | CONCLUSIONS

The current study presented an evaluation of the neuro-fuzzy (NF) systems in estimating daily pan evaporation (E_P) magnitudes in low-altitude stations by using a complete data-scanning procedure, for example, a *k*-fold testing approach. Using data from four low-altitude US weather stations covering a period of 10 years, the NF models were developed and assessed based on local (temporal) and spatial (external) scales. Three input combinations were defined using the available meteorological inputs to feed the NF models. A comparison was carried out between the outcomes of the NF models with neural networks (NN) by using the same materials. The obtained results revealed that the third input combination comprising air temperature, wind speed, solar radiation and humidity records gave promising results for both local and external scales. Accordingly, when no data were available for a target station, the model could be developed using the ancillary data from the feeding station and used in the target station. Nevertheless, the combination comprising air temperature and solar radiation gave accurate results in both scales, which exempts the use of local data when external models fed with exogenous data are available. The present study used data from four low-altitude stations to model daily E_P values. Further investigations might be needed using data from both high and low altitudes to assess the generalizability of the NF (and other models) in order to strengthen the present outcomes.

ORCID

Jalal Shiri https://orcid.org/0000-0002-5726-7924

REFERENCES

Aytek, A. (2008) Co-active neurofuzzy inference system for evapotranspiration modeling. *Soft Computing*, 13(7), 691–700. https://doi.org/10.1007/s00500-008-0342-8.

de Bruin, H.A.R. (1978) A simple model for shallow lake evaporation. *Journal of Applied Meteorology*, 17, 1132–1134.

Brutsaert, W.H. (1982) *Evaporation into Atmosphere*. Springer Netherlands.

Burman, R.D. (1976) Intercontinental comparison of evaporation estimates. *ASCE Journal of Irrigation and Drainage Engineering*, 102, 109–118.

Cahoon, J.E., Costello, T.A. and Ferguson, J.A. (1991) Estimating pan evaporation using limited meteorological observations. *Agricultural and Forest Meteorology*, 55, 181–190.

Chow, V.T., Maidment, D.R. and Mays, L.W. (1988) *Applied Hydrology*. Tata McGraw-Hill Education.

Coppok, D. (1994) *The Borana Plateau of Southern Ethiopia: Synthesis of Pastoral Research, Development and Change, 1980–91*. Addis Ababa: ILCA (International Livestock Centre for Africa).

Cybenco, G. (1989) Approximation by superposition of a sigmoidal function. *Mathematics of Control, Signals, and Systems*, 2, 303–314.

Griffiths, J.F. (1966) Another evaporation formula. *Agricultural and Forest Meteorology*, 3, 257–261.

Hagan, M.T. and Menhaj, M.B. (1994) Training feedforward networks with the Marquaradt algorithm. *IEEE Transactions on Neural Networks*, 6, 861–867.

Haykin, S. (1998) *Neural Networks—A Comprehensive Foundation*, 2nd edition. Upper Saddle River, NJ: Prentice-Hall.

Jang, J.S.R. (1993) ANFIS: adaptive-network-based fuzzy inference system. *IEEE Transactions on Systems, Man, and Cybernetics*, 23(3), 665–685.

Jang, J.S.R., Sun, C.T. and Mizutani, E. (1997) *Neurofuzzy and Soft Computing: A Computational Approach to Learning and Machine Intelligence*. Englewood Cliffs, NJ: Prentice-Hall.

Keskin, M.E., Terzi, O. and Taylan, D. (2004) Fuzzy logic model approaches to daily pan evaporation estimation in Western Turkey. *Hydrological Sciences Journal*, 49(6), 1001–1010.

Kim, S., Shiri, J., Singh, V.P., Kisi, O. and Landeras, G. (2015) Predicting daily pan evaporation by soft computing models with limited climatic data. *Hydrological Sciences Journal*, 60(6), 1120–1136.

Kisi, O. (2006a) Daily pan evaporation modeling using a neuro-fuzzy computing technique. *Journal of Hydrology*, 329, 636–646.

Kisi, O. (2006b) Generalized regression neural networks for evapotranspiration modeling. *Hydrological Sciences Journal*, 51(6), 1092–1105.

Kisi, O. (2006c) Evapotranspiration estimation using feed forward neural networks. *Nordic Hydrology*, 37(3), 247–260.

Kisi, O. and Ozturk, O. (2007) Adaptive neurofuzzy computing technique for evapotranspiration estimation. *Journal of Irrigation and Drainage Engineering*, 133(4), 368–379.

Kisi, O. and Shiri, J. (2010) A comparison of genetic programming and ANFIS in forecasting daily, monthly and daily stremflows. In: *Proceedings of the International Symposium on Innovations in Intelligent Systems and Applications, 21–24 June 2010, Kayseri and Cappadocia, Turkey.* pp. 118–122.

Kisi, O., Pour Ali Baba, A. and Shiri, J. (2012) Generalized neuro-fuzzy models for estimating daily pan evaporation values from weather data. *ASCE Journal of Irrigation and Drainage Engineering*, 138(4), 1–14.

Kohler, M.A., Nordenson, T.J. and Fox, W.E. (1955) *Evaporation from pans and lakes.* Research paper No. 38. Washington D.C.: U.S Weather Bureau.

Kumar, K., Raghuwanshi, N.S. and Singh, R. (2009) Development and validation of GANN model for evapotranspiration estimation. *Journal of Irrigation and Drainage Engineering*, 14(2), 131–140.

Linarce, E.T. (1967) Climate and evaporation from crops. *ASCE Journal of Irrigation and Drainage Engineering*, 93, 61–79.

Mamdani, E.H. and Assilian, S. (1975) An experiment in linguistic synthesis with a fuzzy logic controller. *International Journal of Man–Machine Studies*, 7(1), 1–13.

Marti, P. and Gasque, M. (2010) Ancillary data supply strategies for improvement of temperature-based ETo ANN models. *Agricultural Water Management*, 97, 939–955.

Martí, P., Manzano, J. and Royuela, A. (2011) Assessment of 4-input artificial neural network for ET_0 estimation through data set scanning procedures. *Irrigation Science*, 29, 181–195.

Pour Ali Baba, A., Shiri, J., Kisi, O., FakheriFard, A., Kim, S. and Amini, A. (2013) Estimating daily reference evapotranspiration using available and estimated climatic data by adaptive neuro-fuzzy inference system (ANFIS) and Artificial neural network (ANN). *Hydrology Research*, 44(1), 131–146.

Priestley, C.H.B. and Taylor, R.J. (1972) On the assessment of surface heat flux and evaporation using large-scale parameters. *Monthly Weather Review*, 100(2), 81–92.

Shiri, J. and Kisi, O. (2011a) Comparison of genetic programming with neuro-fuzzy systems for predicting short-term water table depth fluctuations. *Computers and Geosciences*, 37(10), 1692–1701.

Shiri, J. and Kisi, O. (2011b) Application of artificial intelligence to estimate daily pan evaporation using available and estimated climatic data in the Khozestan Province (Southwestern Iran). *ASCE Journal of Irrigation and Drainage Engineering*, 137(7), 412–425.

Shiri, J., Dierickx, W., Pour-Ali Baba, A., Nemati, S. and Ghorbani, M.A. (2011) Estimating daily pan evaporation from climatic data of the state of Illinois, USA using adaptive neuro-fuzzy inference system and artificial neural network. *Hydrology Research*, 42(6), 491–502.

Shiri, J., Marti, P. and Singh, V.P. (2014a) Evaluation of gene expression programming approaches for estimating daily evaporation through spatial and temporal data scanning. *Hydrological Processes*, 28(3), 1215–1225.

Shiri, J., Nazemi, A.H., Sadraddini, A.A., Landeras, G., Kisi, O., Fakheri Fard, A. and Marti, P. (2014b) Comparison of heuristic and empirical approaches for estimating reference evapotranspiration from limited inputs in Iran. *Computers and Electronics in Agriculture*, 108, 230–241.

Stephen, J.C. and Stewart, E.H. (1963) *A comparison of procedures for computing evaporation and evapotranspiration*. Publication 62. Berkeley, CA: International Association of Scientific Hydrology, International Union of Geodynamics and Geophysics.

Takagi, T. and Sugeno, M. (1985) Fuzzy identification of systems and its application to modeling and control. *IEEE Transactions on Systems, Man, and Cybernetics*, 15(1), 116–132.

Wallace, J.S. (1995) Calculating evaporation: resistance to factors. *Agricultural and Forest Meteorology*, 73, 353–366.

Wang, Z., Wu, P., Zhao, X., Cao, X. and Gao, Y. (2014) GANN models for reference evapotranspiration estimation developed with weather data from different climatic regions. *Theoretical and Applied Climatology*, 116, 481–489.

How to cite this article: Shiri J. Evaluation of a neuro-fuzzy technique in estimating pan evaporation values in low-altitude locations. *Meteorol Appl*. 2019; 26:204–212. https://doi.org/10.1002/met.1753